

2017

The role of retromer in adipogenesis

<https://hdl.handle.net/2144/23747>

"Downloaded from OpenBU. Boston University's institutional repository."

BOSTON UNIVERSITY
SCHOOL OF MEDICINE

Thesis

THE ROLE OF RETROMER IN ADIPOGENESIS

BY

HIRA CHAUDHRY

B.S., Fordham University, 2014

Submitted in partial fulfillment of the
requirements for the degree of
Master of Science

2017

© 2017 by
Hira Chaudhry
All rights reserved

Approved by

First Reader

Dr. Kandror Konstantin, Ph.D.
Professor of Biochemistry

Second Reader

Ms. Maryann MacNeil, MA
Instructor of Anatomy and Neurobiology

ACKNOWLEDGMENTS

I would like to thank my Principal Investigator, Dr. Konstantin Kandror of Boston University's School of Medicine Biochemistry Department, for allowing me to work on my thesis his laboratory. I would also like to thank Dr. Xiang Pan, a Post-Doctoral Fellow, who I collaborated with in the following experiments and provided great support in facilitating my work in the laboratory. Finally, I would like to thank the members of Dr. Kandror's laboratory for getting me acquainted with newly learned laboratory techniques.

THE ROLE OF RETROMER IN ADIPOGENESIS

HIRA CHAUDHRY

ABSTRACT

Endocytosis is the process in which a cell engulfs extracellular cargo by creating invaginations within its plasma membrane. The cargo that has entered the cell enters an endosome and then is delivered to either the *trans*-Golgi network for recycling to the plasma membrane or to the lysosome for its degradation (Trousdale & Kim, 2015). Retromer is a peripheral membrane protein complex that plays a key role in sorting of these cargo molecules (Collins, 2008). More specifically, retromer deliver cargo from the endosome to the *trans*-Golgi Network, the process which is called retrograde transport of cargo molecules.

Retromer dysfunction is strongly linked to neurodegenerative diseases such as Alzheimer's and Parkinson's Disease. However, recent Genome Wide Association Studies suggest that a mutation in retromer subunit VPS26a, has been linked to Type II Diabetes (Trousdale & Kim, 2015). A 2016 study published in *The FASEB Journal* attempts to characterize the role of retromer in adipocyte differentiation and insulin-stimulated uptake of glucose through transporter GLUT4 (Yang et al., 2016). The aim of this study is to further investigate the role of retromer in adipogenesis and to determine whether retromer plays a role at the transcriptional level or translational level.

In this study, retromer's VPS35 subunit was knocked down in four mouse 3T3-L1 fibroblast cell lines using the CRISPR-Cas9 approach. These cell lines were

differentiated into mature adipocytes and analyzed by Oil-Red O staining, Western Blotting and quantitative PCR.

The knockdown of retromer produced varying effects on adipocyte differentiation. In two of the knockdown cell lines, adipocyte differentiation was downregulated whereas adipocyte differentiation was upregulated in the other two cell lines. Although the results from Oil-Red O staining and Western Blot analyses complemented each other, results obtained from qPCR were not as straightforward and further analysis is needed to fully comprehend how retromer acts at the transcriptional level of cell differentiation.

Based on the results of this study, retromer is involved in adipogenesis at both the transcriptional and translational level, however it's mechanism of action remains unclear as both cases of impaired differentiation and upregulated differentiation were observed. Further studies are necessary to determine retromer's exact role in adipogenesis.

TABLE OF CONTENTS

TITLE.....	i
COPYRIGHT PAGE.....	ii
READER APPROVAL PAGE.....	iii
ACKNOWLEDGMENTS.....	iv
ABSTRACT.....	v
TABLE OF CONTENTS.....	vii
LIST OF TABLES.....	xi
LIST OF FIGURES.....	x
LIST OF ABBREVIATIONS.....	xi
INTRODUCTION	1
Adipose Tissue: A Dynamic Organ	1
Adipogenesis: From Pre-Adipocyte to Mature Adipocyte.....	1
Glucose Homeostasis.....	5
Function of Retromer.....	7
Structure of Retromer.....	7
The Importance of Sorting Nexins (SNXs).....	10
Retromer’s Interaction with Cargo Proteins.....	12
Diseases Caused by Retromer Dysfunction.....	13
Potential Role of Retromer in Adipogenesis.....	16
CRISPR-CAS9: Genome Editing and Regulating.....	19
How does CRISPR-CAS9 work.....	20

MATERIALS AND METHODS.....	23
3T3-L1 Cell Models of Adipogenesis.....	23
Generation of Lentivirus and Stable VPS35 Knockdown Cell Lines.....	23
Cell Culture and Adipocyte Differentiation.....	25
Oil-Red O Staining and Triglyceride Measurement.....	26
Western Blot Analysis.....	27
Quantitative Polymerase Chain Reaction (qPCR).....	28
Statistical Analysis.....	31
RESULTS.....	32
Successful Knockdown of VPS35.....	32
Triglyceride Measurement.....	33
Protein Levels of VPS35 Knockdown Cell Lines.....	34
mRNA Expression of VPS35 Knockdown Cell Lines.....	36
DISCUSSION.....	39
Level of Differentiation Correlates with Level of Triglyceride Accumulation.....	40
Level of Differentiation Markers Correlates with expression of Differentiation Markers.....	41
Does Level of Differentiation Correlate with mRNA Expression?.....	42
Knockdown of VPS35 Affects the Adipogenesis Process.....	44
Mechanism of Action for Retromer in Adipogenesis Remains Elusive.....	45
Future Implications.....	46
REFERENCES.....	47
CURRICULUM VITAE.....	52

LIST OF TABLES

Table	Title	Page
1	Primers used for qPCR analysis	31
2	Percentage of Protein Levels Expressed	42

LIST OF FIGURES

Figure	Title	Page
1	The Pleiotropic Functions of Adipocytes	2
2	Positive and Negative Transcription Factors of Adipogenesis	3
3	Insulin Signaling Pathway for Glucose Transport Chain	6
4	Structure of retromer assembly	9
5	Intracellular trafficking pathways in mammalian cells	18
6	Mechanism of CRISPR-Cas9	22
7	Successful Knockdown of VPS35	32
8	Level of Differentiation via Triglyceride Accumulation	33
9	Protein Level Expression of Pro-adipogenic Markers in Differentiated Adipocytes	35
10	mRNA Expression of Pro-Adipogenic Markers in Differentiated Adipocytes	36
11	Comparison of Pro-Adipogenic Markers in Relation Triglyceride Accumulation	39

LIST OF ABBREVIATIONS

A β	Amyloid Beta
APP.....	Amyloid Precursor Protein
BAT.....	Brown Adipose Tissue
BCA.....	Bicinchoninic Acid
BS.....	Bovine Serum
cAMP.....	Cyclic Adenosine Mono-Phosphate
Cas9.....	CRISPR-associated protein 9
C/EBP.....	CCAAT/enhancer-binding proteins
CIMPR.....	Cation-Independent Mannose-6-Phosphate Receptor
CRISPR.....	Clustered Regularly Interspaced, Short Palindromic Repeat
crRNA.....	CRISPR RNA
DMEM.....	Dulbecco's Modified Eagles Medium
DMT1-II.....	Divalent Metal Transporter 1 Isoform II
DSB.....	Double-Stranded Break
ESC.....	Embryonic Stem Cell
ER.....	Endoplasmic Reticulum
ETC.....	Endosome-to- <i>trans</i> -Golgi Network Transport Carrier
FBS.....	Fetal Bovine Serum
GLUT4.....	Glucose Transporter 4
GPCR.....	G-Protein Coupled Receptor

gRNA.....	Guide RNA
GSV.....	Glucose Transporter 4 Storage Vesicles
HDR.....	Homology-Directed Repair
HRP.....	Horseradish Peroxidase
iPSC.....	Induced Pluripotent Stem Cell
LDM.....	Low-Density Microsomal
MEF.....	Mouse Embryonic Fibroblasts
MSC.....	Mesenchymal Stem Cell
NHEJ.....	Non-Homologous End-Joining
PAM.....	Proto-spacer Adjacent Motif
PBS.....	Phosphate-buffered Saline
PBST.....	Phosphate-buffered Saline with Tween
PI(3)P.....	Phosphatidylinositol-3-Phosphate
PPAR γ	Peroxisome Proliferator-Activated Receptor γ
P/S.....	Penicillin/Streptomycin
P/S/G.....	Penicillin/Streptomycin/Glutamine
PVDF.....	Polyvinylidene Difluoride
PX.....	Phosphoinositide-Binding
qPCR.....	Quantitative Polymerase Chain Reaction
RIPA.....	Radio-immunoprecipitation Assay
SDS.....	Sodium Dodecyl Sulfate
SDS-PAGE.....	Sodium Dodecyl Sulfate Polyacrylamide Gel Electrophoresis

SNX.....Sorting Nexin
TG.....Triglyceride
TGN.....*trans*-Golgi Network
tracrRNA.....Transactivating CRISPR RNA
VPS.....Vacuolar Protein Sorting
WAT.....White Adipose Tissue

INTRODUCTION

ADIPOSE TISSUE: A DYNAMIC ORGAN

Adipose tissue is a dynamic organ that carries out several important physiological functions. There are two types of adipose tissue: White Adipose Tissue (WAT) and Brown Adipose Tissue (BAT). WAT accounts for the majority of fat in adults and is responsible for storage of lipids. BAT is responsible for generation of heat in the process of non-shivering thermogenesis (Cold Spring Harb Perspect Biol 2012;4:a008417). For the purposes of this study, when referring to adipose tissue, we will only consider WAT.

Since the discovery of leptin, a secretory hormone that functions exclusively in adipocytes and mediates satiety through receptors located in the hypothalamus, it has been concluded that WAT plays an active role in energy metabolism in a variety of ways. For example, processes associated with lipid metabolism are best exemplified by the storage and release of fatty acids for important processes such as myocardial contraction. Secretion of glycerol and fatty acids from adipocytes also plays an important role in hepatic and peripheral glucose metabolism. In addition, adipose tissue, skeletal muscle and cardiac muscle are the only known tissues to express and regulate insulin-dependent glucose transporter, GLUT4, which facilitates the entry of glucose into these cells and out of circulation post-prandially. The pleiotropic functions of adipose tissue are also illustrated in Figure 1 (Morrison & Farmer et al., 2000; Farmer et al., 2006).

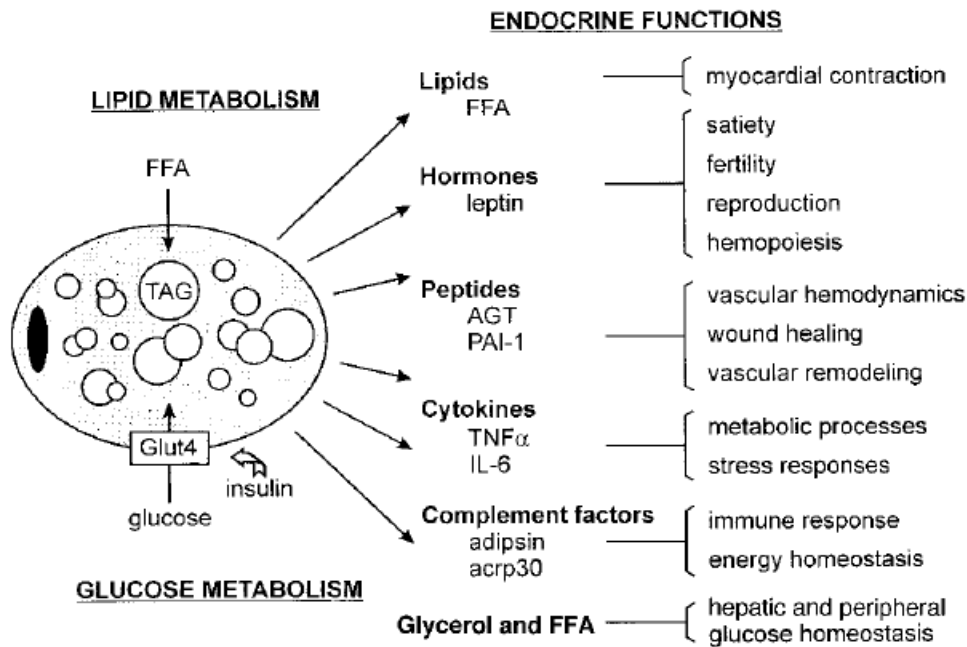


Figure 1. The pleiotropic functions of adipocyte (Morrison & Farmer et al., 2000).

ADIPOGENESIS: FROM PRE-ADIPOCYTE TO MATURE ADIPOCYTE

Stem cells are cells capable of renewing themselves through cell division and can differentiate into multi-lineage cells. Stem cells are categorized into three categories: embryonic stem cells (ESCs), induced pluripotent stem cells (iPSCs) and adult stem cells. Mesenchymal stem cells (MSCs) are adult stem cells that are non-hematopoietic and multipotent with the capacity to differentiate into mesodermal lineage such as osteocytes, chondrocytes and adipocytes (Ullah, Subbarao, & Rho et al., 2015). The differentiation of MSCs into mature adipocytes requires key transcription factors which include peroxisome proliferator-activated receptor γ (PPAR γ), CCAAT/enhancer-binding

proteins (C/EBPs) and other transcription factors (Cold Spring Harb Perspect Biol 2012;4:a008417; Farmer et al., 2006; X. Ma, Lee, Chisholm, & James et al., 2015).

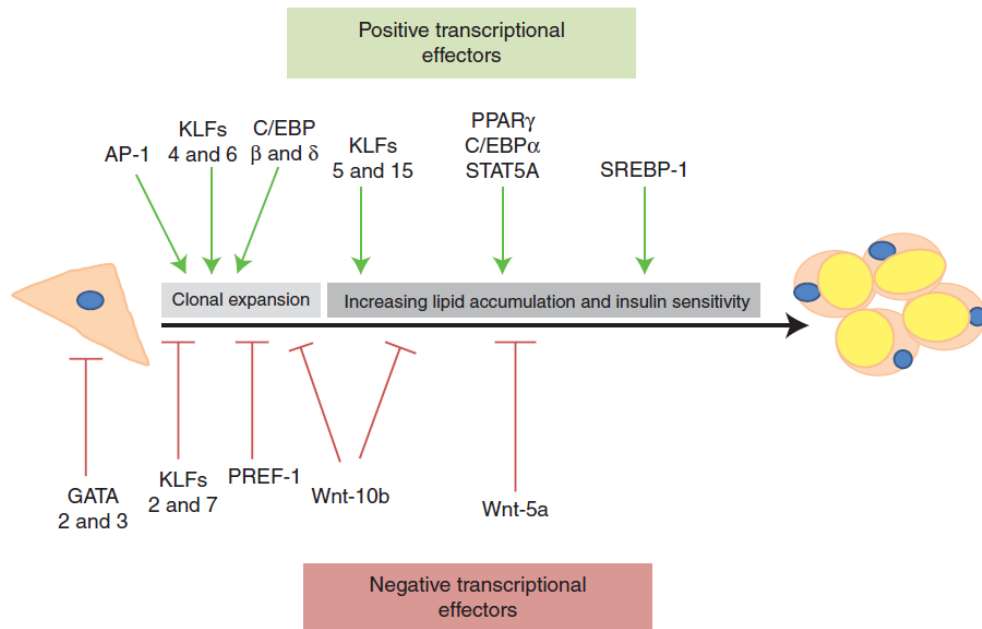


Figure 2. Positive and negative transcription factors of adipogenesis (Cold Spring Harb Perspect Biol 2012;4:a008417).

Although there are many transcription factors that promote adipogenesis, PPAR γ and C/EBP α are considered the master regulators of adipogenesis which has been supported by overwhelming evidence obtained from *in vivo* and *in vitro* studies. Through gain-of-function studies in which PPAR γ was ectopically expressed in non-adipogenic mouse fibroblasts, it was demonstrated that PPAR γ alone can initiate adipogenesis (Cold Spring Harb Perspect Biol 2012;4:a008417; Farmer et al., 2006). In studies using

PPAR γ knockout mouse cell lines, these cells failed to develop into adipocytes whereas wild-type cells gave rise to fully functional adipocytes (Farmer et al., 2006; Hammarstedt, Andersson, Sopasakis, & Smith et al., 2005; Morrison & Farmer et al., 2000; Siersbæk, Nielsen, & Mandrup et al., 2010; Rosen et al., 1999).

The role of C/EBP α as a master regulator of adipogenesis was also observed through gain-of-function studies in cultured cells as well as in knockout mice. Ectopic expression of C/EBP α in fibroblastic cells could induce adipogenesis. Furthermore, C/EBP α knockout mice died shortly birth due to their inability to produce glucose, as C/EBP α is necessary for gluconeogenesis to occur in the liver. These knockout mice were also incapable of producing WAT.

Interestingly, PPAR γ can induce adipogenesis in C/EBP α -deficient MEFs (mouse embryonic fibroblasts); however, C/EBP α cannot induce adipogenesis in PPAR γ -deficient MEFs. This observation suggests that PPAR γ and C/EBP α operate in a single-direction pathway in which PPAR γ is the dominant factor in initiating adipogenesis.

Other important transcription factors are C/EBP β and C/EBP γ , which are expressed earlier than C/EBP α during adipogenesis in 3T3-L1 cells, a mouse fibroblast model used to study adipogenesis, and are responsible for the expression of C/EBP α . Using 3T3-L1 pre-adipocytes, the ectopic expression of C/EBP β and C/EBP γ induced the expression of C/EBP α in the absence of extracellular hormones. Furthermore, the expression of C/EBP β and C/EBP γ into 3T3-L1 fibroblasts can initiate adipogenesis without stimulating the expression of C/EBP α .

In terms of the effect of C/EBP β and C/EBP γ on PPAR γ expression, ectopic expression of C/EBP β and C/EBP γ induces PPAR γ expression which facilitates the conversion of pre-adipocytes into mature adipocytes. However, there is no C/EBP α expression if PPAR γ is not expressed. Additional studies have shown that retroviral expression of C/EBP β in PPAR γ -deficient MEFs is incapable of stimulating C/EBP α expression. Therefore, it can be concluded that in the principal pathway of adipogenesis, C/EBP β and C/EBP γ induce PPAR γ expression and PPAR γ in conjunction with these C/EBPs induces C/EBP α expression (Morrison & Farmer et al., 2000; Farmer et al., 2006; Cold Spring Harb Perspect Biol et al., 2012;4:a008417; Guo, Li, & Tang et al., 2015). Activation of C/EBP β and PPAR γ result in gene expression of downstream proteins, such as sortilin and GLUT4, that ultimately allow mature adipocytes to participate in energy metabolism processes (Yang et al., 2016).

GLUCOSE HOMEOSTASIS

Insulin, a peptide hormone, is ultimately responsible for maintaining glucose homeostasis throughout the body. Insulin achieves glucose homeostasis by stimulating signaling cascades that tightly control glucose transporter 4 (GLUT4) trafficking in a spatially and temporally dependent manner.

When insulin is not present, GLUT4 is stored within specialized intracellular compartments called glucose transporter 4 storage vesicles, or GSVs. However, after a meal, insulin is secreted from pancreatic β cells and interacts with the insulin receptor on insulin-responsive tissues, such as adipose and skeletal muscle tissues. This activates a

cascade of signaling events that ultimately promotes the translocation of the GSVs to the plasma membrane of these cells. The translocation of GLUT4 to the plasma membrane then allows for glucose to enter the cells from the bloodstream. Any disruptions in insulin signaling and GLUT4 trafficking pathways can result in insulin resistance and impaired glucose uptake, usually resulting in the development of Type II Diabetes.

The formation of GSVs is a highly regulated process in which many transmembrane proteins, such as GLUT4, insulin-responsive aminopeptidase (IRAP) and sortilin, a member of the vacuolar protein sorting (Vps) 10 family of transmembrane receptors, are involved. These transmembrane proteins are selectively targeted to enter GSVs and aid in the process of recruiting GLUT4 to the plasma membrane.

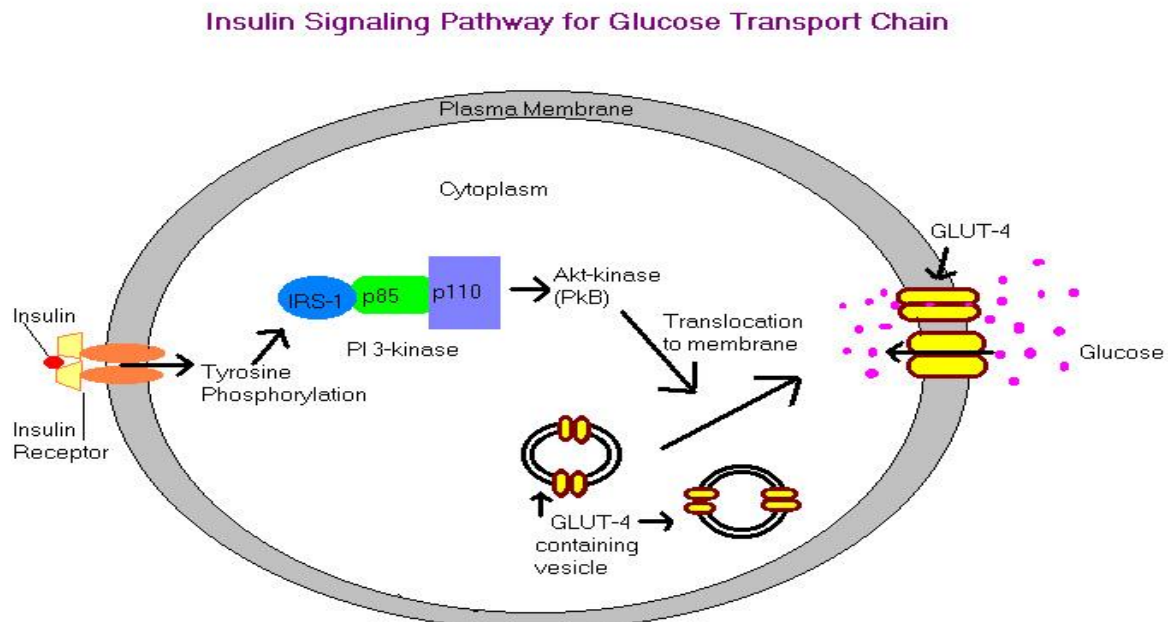


Figure 3. Regulation of Glucose Transport by insulin Simplified Mechanism of Insulin-stimulated Glucose Uptake in Cell (“Insulin Signaling Transduction Pathway”).

IRAP and sortilin both interact with GLUT4 and are essential for the formation of the GSVs. After translocation to the PM, these GSV components must be recycled by endocytosis and sorted within endosomal compartments. It is believed that a protein complex called Retromer plays a central role in aiding the intracellular trafficking and sorting of transmembrane proteins, such as IRAP and sortilin, within endosomal compartments (Bogan & Kandror et al., 2010; Shi & Kandror et al., 2005; Yang et al., 2016).

FUNCTION OF RETROMER

Endocytosis is the process in which a cell engulfs extracellular cargo by creating invaginations within its plasma membrane. The cargo that has entered the cell enters an endosome and then is delivered to either the *trans*-Golgi network for recycling to the plasma membrane or to the lysosome for its degradation (Trousdale & Kim et al., 2015). Retromer is a multi-protein complex that associates with the cytosolic face of endosomes where it functions to recycle various cargo, such as receptors, transporters, adhesion molecules and other proteins to the TGN, or retrograde transport. Once modified at the TGN, cargo is recycled back to the plasma membrane (Collins et al., 2008; Lucas et al., 2016; Mukadam & Seaman et al., 2015; Wu, Hamid, Shin, & Chiang et al., 2014; Wu et al., 2014).

STRUCTURE OF RETROMER

Although the structure of retromer still remains elusive, there have been attempts to uncover this mystery. Retromer consists of two distinct parts: a core complex containing the subunits VPS35, VPS26 and VPS29 (also referred to as the cargo-loading complex) and an associated dimer of proteins from the sorting nexin (SNX) protein

family. It was previously thought that among the subunits of retromer's cargo-loading complex, VPS35 was the major cargo-binding subunit. Both VPS35 and VPS29 associated with the phosphatidylinositol-3-phosphate, or PI(3)P-binding SNX complexes and interaction allowed for the endosomal recruitment of retromer (Collins et al., 2008).

Despite the widely held view that the VPS26-VPS35-VPS29 retromer trimer is responsible for cargo recognition, there is currently no evidence to support this notion. A recent 2016 study published in *CellPress Journal* attempted to elucidate the true structure of retromer using X-ray crystallography techniques. It was concluded that the overall complex has a T-shaped structure with VPS26 and the N-terminal portion of VPS35 (VPS35N) corresponding to both sides of the horizontal bar and SNX3 to the vertical bar. The C-terminal lobe of VPS26 (VPS26C), previously thought to contact VPS35, interacts through strands $\beta 15$, $\beta 16$ and the connecting loop with helices $\alpha 4$, $\alpha 5$, $\alpha 6$ and $\alpha 8$ on the convex side of VPS35 α -solenoid. SNX3 binds simultaneously through its N-terminal tail and PX (phosphoinositide-binding) domain to VPS26C and VPS35N. The PI(3)P-binding pocket on the SNX3 PX domain occurs on the opposite side of the VPS26-VPS35-interaction, consistent with the role of SNX3 in retromer recruitment to endosomal membranes. The overall structure of the retromer complex is depicted in Figure 4 below.

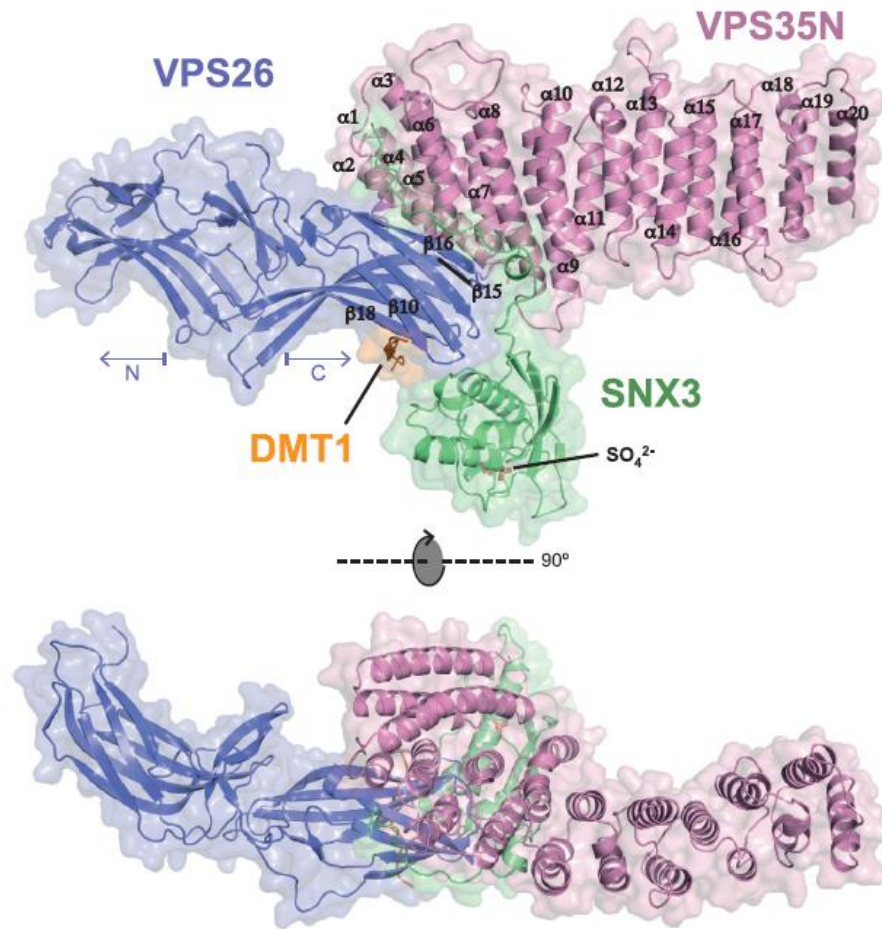


Figure 4. Structure of retromer assembly. Overall crystal structure of retromer complex in two orthogonal views. In top view, the 20 α -helices that make up the solenoid structure of VPS35N (N-terminal side of VPS35) and four β -strands from C-terminal of VPS26 are labeled. Two sulfate ions (SO_4^{2-}) indicate the PI(3)P-binding pocket on SNX3 (Lucas et al., 2016).

VPS26A and VPS26B, paralogs of VPS26, bind to VPS35 at its highly conserved $^{106}\text{PRLYL}^{110}$ for which the two VPS26 paralogs compete. Binding of VPS26 and VPS35 is through a central hydrophobic core dominated by P247 of VPS26, I104 and M136 of VPS35 and an extended hydrogen-bond network (Lucas et al., 2016). It has been shown that the double mutation P245S/R247S in VPS26B (analogous to P247S/R249S in

VPS26A) prevented its incorporation into retromer *in vivo* and *in vivo* (Collins et al., 2008). These mutations destabilize VPS26 C-domain's hydrophobic core. Furthermore, crystal structures of VPS35N alone and in complex with VPS26A show that the ¹⁰⁶PRLYL¹¹⁰ sequence in VPS35 is at a buried position in α -helix 5, serving as a major structural scaffold for stabilization of the surrounding helical solenoid. The only side chain that sticks out to the surface is R107, which interacts with E34 and Y233 of VPS26A. Therefore, it is likely that any mutations to R107 affect interaction with VPS26 while other mutations within the ¹⁰⁶PRLYL¹¹⁰ sequence have a destabilizing effect that abolishes binding (Jia et al., 2016; Lucas et al., 2016; Seaman et al., 2012; Zhao et al., 2007).

THE IMPORTANCE OF SORTING NEXINS (SNXs)

Sorting nexins (SNXs) are a conserved class of proteins defined by a phosphoinositide-binding phox homology (PX) domain that play a role in membrane trafficking at endosomes. Many SNXs play a role, directly or indirectly, in the recognition of cargo proteins (Bean, Davey, & Conibear et al., 2017). The SNX family can be divided into five subfamilies: the SNX-PX, SNX-BAR (Bin/Amphiphysin/Rvs), SNX-FERM (protein 4.1/ezrin/radixin/moesin), SNX-PXA-RGS-PXC and SNX-MIT. In regards to retromer function, members of the SNX-BAR subfamily as well as SNX27 of the SNX-FERM subfamily and SNX3 of the SNX-PX subfamily are of utmost importance.

SNX-BAR members contain a C-terminal BAR domain in addition to the SNX-PX domain. Their BAR domains possess a concave surface with basic residues that associate with membranes through electrostatic interactions. It is believed that this curved structure allows BAR domains to optimally bind to and stabilize curved membranes. The SNX-PX domain allows for simultaneous detection of phosphoinositide-binding sites at these curved membranes. The SNX-BAR subcomplex, which consists of SNX1, SNX2, SNX5, SNX6 and SNX32, associates with mammalian retromer. This SNX-BAR-retromer complex is thought to bend the endosome membrane to form tubular-carriers for retromer cargo (Gallon & Cullen et al., 2015), which is consistent with the older model of retromer function described in Figure 4 (Collins et al., 2008). SNX-BAR subcomplex interactions with the dynein-dynactin minus-end-directed motor complex of the microtubule cytoskeleton of ETCs allows transport of carriers containing retromer cargo (Cullen & Korswagen et al., 2012; Gallon & Cullen et al., 2015).

SNX's from the SNX-FERM subfamily contain an atypical FERM domain C-terminal to the SNX-PX domain characteristic of SNXs. SNX27 is unique because not only does it contain a FERM domain, but also a PDZ domain, a type of protein interaction domain of approximately 90 amino acids, that binds to proteins at its C-terminus. The PDZ domain of SNX27 binds to VPS26 (both VPS26A and VPS26B paralogues) through a series of interactions with residues in the groove between the two lobes of VPS26. The β 3- β 4 loop of SNX27 allows it to simultaneously engage with both PDZ-binding motif and retromer, acting as sorting signals in the cytoplasmic tails of

cargo proteins, thereby linking cargo proteins to the endosomal trafficking machinery for recycling to the plasma membrane. In this way, SNX27 acts as a cargo adaptor for retromer, creating a more diverse pool of cargo that is dependent on retromer for endosome-to-plasma membrane trafficking (Clairfeuille et al., 2016; Gallon & Cullen et al., 2015).

Recently, SNX3 of the SNX-PX subfamily was shown to help recruit the retromer complex to endosomes in yeast, suggesting SNX3 not only possess cargo-recognition properties, but also enhances retromer complex recruitment to endosomes (Bean, Davey, & Conibear et al., 2017). Wntless, a transmembrane-domain protein that is required for the transport of Wnts, lipid-modified glycoproteins secreted by cells to act as short-range signals and long-range morphogens vital to development and tissue homeostasis, relies on SNX3-retromer complex for its retrograde transport to the plasma membrane. SNX3 is the perfect candidate for this task because it contains a PI(3)-P binding site and Wntless is dependent on phosphoinositide for its retromer-dependent sorting. SNX3-retromer regulates endosome-to-TGN retrieval of Wntless (Cullen & Korswagen et al., 2012; Gallon & Cullen et al., 2015; Bean et al., 2017).

RETROMER'S INTERACTION WITH CARGO PROTEINS

It was previously assumed that primary binding of retromer to cargo proteins occurred primarily through the VPS35 subunit (Collins et al., 2008). However, in light of recent studies, there is reason to believe that VPS26A plays an important role in binding to cargo, as the overall structure of VPS26A exhibits several conformational changes

when complexed with other proteins. The most notable conformational change in VPS26 is the outward movement of its β 10 strand, creating a hydrophobic pocket between strands β 10 and β 18. This hydrophobic contains an electron density which corresponds to a foreign C-terminal sequence QPEMGLV from a symmetrically related VPS26 molecule.

Interestingly, this sequence fits the \emptyset X(L/M) consensus motif (where \emptyset represents an aromatic amino acid) for cargo selection by retromer and strongly resembles the recycling signal, $_{551}$ QPELYLL $_{557}$, of the divalent metal transporter 1 isoform II (DMT1-II), a known retromer cargo. The central part of the interaction corresponds to L557 of DMT1-II, which is completely buried within the hydrophobic pocket between strands β 10 and β 18 of VPS26. The recycling signal of DMT1-II creates an extensive network of hydrogen bonds and hydrophobic interactions engaging both SNX3 and VPS26 (Jia et al., 2016; Lucas et al., 2016; Seaman et al., 2012; Zhao et al., 2007). SNX27-retromer has also been shown to facilitate the binding of VPS26 to DMT1-II (Steinberg et al., 2013).

DISEASES CAUSED BY RETROMER DYSFUNCTION

Retromer has been implicated to play a role in the pathology of neurodegenerative diseases such as Alzheimer's and Parkinson's disease. Although the specifics of the progression of these fairly widespread diseases still remains uncertain, retromer activity has been identified as contributors to these diseases and is a potential avenue for learning more about retromer's function in human disease pathology.

Alzheimer's disease is a neurodegenerative disease characterized by amyloid beta ($A\beta$) plaques, aggregates of $A\beta$ protein in brain tissue, resulting in loss of cell function in the brain. $A\beta$ proteins are the result of improper cleavage of cellular amyloid precursor protein (APP). APP is a plasma membrane protein produced in the endoplasmic reticulum (ER) of cells and is targeted to the plasma membrane via the secretory pathway. Afterwards, it is endocytosed and recycled to the plasma membrane. In the endosome, APP is cleaved by α -secretase and then is trafficked to the TGN via retrograde transport and then is placed into the plasma membrane. At the plasma membrane, APP is further cleaved by γ -secretase.

BACE1, a known retromer cargo, is recycled between the endosome and TGN via retromer and is capable of improperly cleaving APP. When retromer function is impaired, BACE1 and APP are inefficiently recycled, resulting in a build-up of BACE1 in the endosome and APP residing in the endosome longer than usual. Thus, there is more APP being processed by BACE1. When the improperly cleaved APP is trafficked to the plasma membrane, it is further processed by γ -secretase and the resulting protein produced is $A\beta$.

The knockdown of VPS35 in retromer is thought to play a role in the pathology of Alzheimer's as lower levels of VPS35 are detected in tissue samples of patients. Furthermore, knockdown studies of VPS35 have shown that reduced levels of VPS35 is positively correlated with the production of $A\beta$. Clinically, detecting reduced levels of VPS35 could be indicative of the onset of Alzheimer's disease (Kimura et al., 2016;

Sadigh-Eteghad, Askari-Nejad, Mahmoudi, & Majdi et al., 2016; Trousdale & Kim et al., 2015; Zhang, Tan, Yu, & Tan et al., 2016).

Parkinson's disease also displays strong links to retromer dysfunction in neurons. Mutation of the VPS35 gene, p.D620N, has been linked to familial inherited and idiopathic forms for Parkinson's disease. The result of this mutated gene is unclear as many different effects are observed. For instance, in some cases complete loss of function of retromer is observed whereas in other cases, mutations result in loss of retrograde transport to the TGN or defective auto-phagosome formation.

Mutation of p.D620N can also lead to the formation of enlarged endosomes which are misdirected to the nucleus area, which has been confirmed using patient tissue sample. This gene mutation can also result in the accumulation of Lewy bodies, the hallmark of Parkinson's disease. Lewy bodies form when excess cellular α -synuclein oligomerizes in cells and is excreted to the extracellular matrix. α -synuclein is normally degraded by the enzyme Cathepsin D, a known cargo of the cation-independent mannose-6-phosphate receptor (CIMPR) which is in turn a known cargo for retromer. Cathepsin D is synthesized in the ER and then trafficked to the Golgi, where it binds to CIMPR to be transported to the endosome.

Upon its arrival, Cathepsin D releases from CIMPR and enters the lysosome where it becomes active and degrades α -synuclein. When the function of retromer is compromised, Cathepsin D cannot reach the lysosome and α -synuclein cannot be properly degraded. Excess α -synuclein results in the formation of Lewy Bodies, interrupting neuronal homeostasis and the onset of Parkinson's disease. Although

retromer typically functions in the retrograde transport of cargo, in this scenario retromer is facilitating the degradation of α -synuclein. The authors of this study do not comment on this action of retromer.

A third effect of this mutation is cells with dysfunctional retromer have been shown to mistarget the proteins DMT1-II and Wntless to the lysosome. DMT1-II deficiencies have been linked to iron accumulation in patients with Parkinson's disease. Furthermore, Wntless is necessary for many neuronal signaling functions, including development of cells and cell-to-cell communication (Trousdale & Kim et al., 2015). Although recent studies have demonstrated VPS26 to be the cargo adaptor in the retromer complex, VPS35N provides structural stability for VPS26. Therefore, it can be suggested that disruptions in VPS35 stability hinders VPS26's ability to bind to cargo such as DMT1-II and Wntless (Gallon & Cullen et al., 2015; Lucas et al., 2016).

POTENTIAL ROLE OF RETROMER IN ADIPOGENESIS

Although the bulk of diseases linked to retromer dysfunction are largely neurodegenerative, a non-neural pathology Diabetes Mellitus has been shown to be associated with retromer, although there is no direct evidence linking retromer to its causation. Genome-wide association studies have identified a genetic variation within the VPS26A loci that is associated with Type II Diabetes in a South Asian population. In addition, the VPS10-family receptor SorCS1 has been linked to both Type I and Type II Diabetes. It remains unclear what role these genetic variations play in the onset of Type I and Type II Diabetes (Kooner et al., 2011; Trousdale & Ki et al., 2015).

A study conducted by the Department of Cell Biology at Gunma University in Japan has demonstrated that prolonged blood insulin levels down-regulates the expression and trafficking of GLUT4 to the plasma membrane of adipocytes by inhibiting retromer through phosphorylation. In 3T3-L1 adipocytes, GLUT4 levels were reduced by approximately 60% upon knockdown of VPS26 of retromer and increased upon overexpression of VPS26 and/or VPS35, although insulin down-regulated GLUT4 to the same level as in cells in the basal state. This demonstrates a potential role of retromer in the maintenance of GLUT4 levels in the basal state by retrieving GLUT4 from the endosome-to-lysosome degradative flow. This also suggests that insulin promotes retromer dissociation from the low-density microsomal (LDM) membranes of adipocytes, facilitating the degradation of GLUT4 in lysosomes. Insulin upregulates the activity of protein kinase CK2. CK2 inhibits VPS35 through phosphorylation, which disrupts VPS35's interaction with sortilin. VPS35 subunits with a mutation in the CK2 phosphorylation motif were resistant to insulin-induced dissociation from LDM membrane and its overexpression prevented GLUT4 down-regulation by insulin (Flores-Riveros, McLenithan, Ezaki, & Lane et al., 1993; J. Ma, Nakagawa, Kojima, & Shibata et al., 2014; Maier & Gould et al., 2000).

According to another recent experiment published in *The FASEB Journal*, conducted by the Yang Laboratory at the Institute for Molecular Biosciences in Australia, a correlation between level of retromer expression and level of adipogenesis was observed using wild-type mature adipocytes with functional retromer complexes and adipocytes with VPS35 knock down. Using Western Blot analysis the authors found that,

PPAR γ , a crucial transcription factor that promotes adipocyte differentiation, was expressed at lower levels in adipocytes upon knockdown of VPS35. Similarly, C/EBP β expression was also decreased in these knockdown cells.

However, when C/EBP β and PPAR γ are under expressed, this results in lower levels of sortilin and GLUT4 protein levels in adipocytes. Due to the fact that sortilin is a cargo protein for retromer, inadequate levels of retromer lead to inefficient recycling of sortilin from early endosomes. As a result, degradation of sortilin occurs as early endosomes mature into late endosomes/lysosomes. With reduced sortilin levels in adipocytes, GSV formation will be impaired, resulting in lower protein levels of GLUT4. This impairs the adipocytes' ability to uptake glucose when stimulated by insulin. This could ultimately result in insulin resistance and down the line, Type II Diabetes (Yang et al., 2016).

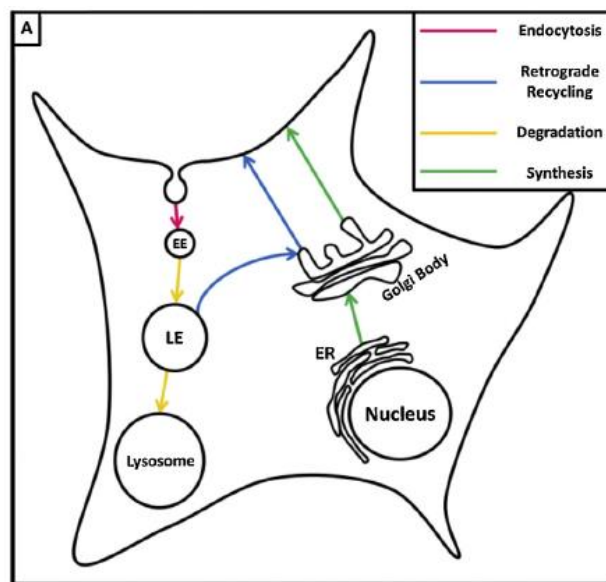


Figure 5. Intracellular trafficking pathways in mammalian cells. Retromer is responsible for trafficking proteins such as sortilin from late endosome (LE) to TGN. Sortilin and IRAP can then interact with GLUT4 in GSVs for recruitment to the plasma

membrane. GLUT4 is then endocytosed by early endosomes (EE) and either degraded in lysosomes or recycled to TGN (Trousdale & Kim, 2015).

CRISPR-CAS9: GENOME EDITING AND REGULATING

The introduction of targeted genomic sequence changes into living cells and organisms has become a powerful tool for biological research and can potentially provide scientists with insight on how to better therapeutically target genetic diseases. The use of Clustered Regularly Interspaced, Short Palindromic Repeat (CRISPR) technology has become an important new approach for generating RNA-guided nucleases, such as Cas9, with customizable specificities. These nucleases are used to rapidly, easily and efficiently modify endogenous genes in a variety of cell types and to ultimately, genetically manipulate cells and living organisms.

Targeted genome editing using customized nucleases provides a general method for introducing targeted deletions, insertions, frameshift knockout mutations and other precise sequence changes in a variety of organisms and cell types. A crucial first step for targeted genome editing is the creation of a DNA double-stranded break (DSB) at the genomic locus to be modified. DSBs induced by nucleases can be repaired using one of two different methods: non-homologous end-joining (NHEJ) and homology-directed repair (HDR). NHEJ is advantageous when the desire is to efficiently introduce insertion/deletion mutations of various lengths, which ultimately disrupts the translational reading frame of a coding sequence or the binding sites of *trans*-acting factors in promoters or enhancers. HDRs are favorable when introducing specific point mutations

or inserting desired sequences through recombination of the target locus with exogenous DNA “donor templates.”

Early methods for modifying specific genomic sequences with DSB-inducing nucleases rely on protein-based systems with customizable DNA-binding specificities, such as zinc finger nucleases and transcription activator-like effector nucleases. A more recent method based on a bacterial CRISPR-associated protein 9 (Cas9) nucleases from *Streptococcus pyogenes* has been developed. This method is thought to be more flexible because it depends on RNA as the moiety that targets the nuclease to a desired DNA sequence. Furthermore, RNA-guided nucleases use simple base-pairing rules between an engineered RNA and the target DNA site (Ding, Li, Chen, & Xie et al., 2016; Sander & Joung et al., 2014; Wang, Huang, Fang, Zhang, & Wang et al., 2016).

HOW CRISPR-CAS9 WORKS

CRISPR systems are adaptable immune mechanisms used by many bacteria to protect themselves from foreign nucleic acids, such as viruses and plasmids. Naturally occurring CRISPR-Cas9 systems incorporate sequences from invading DNA between CRISPR repeat sequences encoded as arrays within the bacterial host genome.

Transcripts from the CRISPR repeat arrays are processed into CRISPR RNAs, or crRNA. Each crRNA contains a variable sequence transcribed from the invading DNA, known as the “proto-spacer” sequence, and part of the CRISPR repeat. Each crRNA hybridizes with a second RNA, known as the transactivating CRISPR RNA, or tracrRNA. These two RNAs form a complex with the Cas9 nuclease. The proto-spacer-encoded portion of

the crRNA directs Cas9 to cleave complementary target-DNA sequences, if they are adjacent to short sequences known as proto-spacer adjacent motifs (PAMs).

When reproducing this mechanism in the laboratory, two components must be introduced into and/or expressed in cells or an organism to editing its genome: the Cas9 nuclease and a guide RNA (gRNA), which is a fusion of a crRNA and tracrRNA. The twenty nucleotides at the 5' end of the gRNA (corresponding to the proto-spacer portion of the crRNA) direct Cas9 to a specific target DNA site using standard RNA-DNA complementarity base-pairing rules. These target sites must lie immediately 5' of a PAM sequence that matches the canonical form 5'-NGG (N representing any sequence of nucleotides). Thus, Cas9 nuclease activity can be directed at any DNA sequence of the form N₂₀-NGG simply by altering the first 20 nucleotides of the gRNA to correspond to the target DNA sequence (Ding, Li, Chen, & Xie, 2016; Sander & Joung, 2014; Wang, Huang, Fang, Zhang, & Wang, 2016).

MATERIALS AND METHODS

3T3-L1 CELL MODEL OF ADIPOGENESIS

There are two classes of models that are widely used to study adipogenesis: the first group includes pluripotent fibroblasts, fibroblasts with the ability to proliferate rapidly while maintaining the ability to differentiate into various types of cell lines myocytes, chondrocyte and adipocytes and the second group includes fibroblast-like pre-adipocytes that are committed to differentiating into adipocytes.

A 3T3-L1 cell line, which falls under this second group, was used for the following experiments. With the introduction of mitogens and hormonal agents, such as insulin, glucocorticoids and other agents that lead to an increase in cAMP (cyclic Adenosine Mono-phosphate), a cascade of transcriptional events ensue, allowing these cells to differentiate into a homogenous population of mature adipocytes that are morphologically and biochemically similar to adipocytes *in situ* (Cold Spring Harb Perspect Biol 2012;4:a008417; Morrison & Farmer et al., 2000; Farmer et al., 2006; Yamanaka et al., 2008).

GENERATION OF LENTIVIRUS AND STABLE VPS35 KNOCKDOWN CELL LINES

The lentivirus used to transfect wild-type 3T3-L1 cells to form stable VPS35 knockdowns was produced using human embryonic kidney cells HEK293T. Lentiviral particles were created by growing HEK293T cells in 10% FBS/DMEM (Fetal Bovine

Serium/Dulbecco's Modified Eagle's Medium) without antibiotics (no penicillin or streptomycin). The cells were incubated at 37°C and 10% CO₂ overnight.

In polypropylene microfuge tubes, a cocktail containing 3µg lentiCRISPRv2 plasmid, 2.5 µg psPAX2 packaging plasmid, 1.5 µg VSV-G envelope plasmid and 250µL of serum-free OPTI-MEM, was prepared for each transfection. The following gRNAs were constructed into lentiCRISPRv2 plasmid separately and used for stable knockdown of VP35:

gRNA1: AGTTTTTCCTGCTCATCCTG

gRNA2: GAGCTCTCCAAGCATATTGG

gRNA3: TGATGAACTGCACTACTTGG

gRNA4: GATTTGGTAGAAATGTGCCG

Where V-5-1 and V-5-2 cell lines contained gRNA4, V-2-2 cell line contained gRNA1 and V-M cell line contained all four gRNAs.

A master mix of lipofectamine 2000 transfection reagent was prepared in serum-free OPTI-MEM such that each reaction utilizes 20µl lipofectamine 2000 + 250 µL OPTI-MEM. The master mix was mixed the cocktails in the microfuge tubes and incubated at room temperature for 30 minutes. This mix was then added dropwise to the HEK293T cells and incubated at 37°C and 5% CO₂ for 7.5 hours.

Afterwards, the medium was replaced with 10% FBS/DMEM containing 5mL P/S (penicillin/streptomycin). Cells were incubated at 37°C and 5% CO₂ for 48 hours. Cell

medium was then filtered by 0.45 µm filter and transferred to a polypropylene storage tube, containing the lentiviral particles.

The lentiviral particles were introduced to wild-type 3T3-L1 fibroblasts in serum-free medium containing 6 µg/ml Polybrene. The cells were incubated at 37°C and 10% CO₂ for 24 hours after which medium was replaced by 10% BS/DMEM containing P/S/G for an additional 48 hours. Transduced cells were then subjected to puromycin selection to test for puromycin resistance. Titer cells to 96-well plates and use 4 µg/ml puromycin to select the single colonies.

CELL CULTURE AND ADIPOCYTE DIFFERENTIATION

3T3-L1 fibroblasts and the four knockdown single colony cell lines, V-5-1, V-5-2, V-2-2, V-M were cultured in high-glucose DMEM with L-glutamine. The DMEM was supplemented with 10% bovine serum (BS) (GibcoBRL), 5mg/ml P/S/G (penicillin/streptomycin/glutamine) (GibcoBRL). Cell lines were then maintained 10% CO₂ at 37°C. When reaching confluency, the fibroblasts were ready to be differentiated.

In preparation for differentiating fibroblasts into adipocytes, the following fresh solutions were prepared: 11mg of 3-isobutyl-1-methylxanthine (IBMX) (Sigma-Aldrich) dissolved in 1mL of 0.5N KOH, resulting in a final concentration of 0.11g/mL, which was filtered and sterilized through a 0.22µm syringe filter, 167µM Insulin stock (1mg/mL) (Sigma-Aldrich) in 0.02M HCl, which was also filtered and sterilized through a 0.22µm syringe filter, and 10mM of Dexamethasone (Sigma-Aldrich) in 100% Ethanol.

To the required volume of 10% FBS/DMEM (same culture medium as fibroblasts, except 10% BS is replaced with 10% FBS) needed to induce differentiation in a cell plate, the following ratios of solutions were added: 1:100 IBMX, 1:1000 Insulin, 1:1000 Dexamethasone. This is the differentiation medium prepared in FBS/DMEM.

The BS/DMEM medium was withdrawn and replaced with the FBS/DMEM medium containing the differentiation medium. Cells were maintained under the same conditions (10% CO₂ at 37°C) for three days upon initiation of differentiation (Day 0-2).

After the third day of initiating differentiation (Day 2), the differentiation culture medium was replaced with only FBS/DMEM and cell lines were maintained 10% CO₂ at 37°C. The DMEM medium was replaced with fresh DMEM every other day until cell differentiation was complete. Differentiated adipocytes were ready for experimental use by Days 7-10.

OIL RED O STAINING AND TRIGLYCERIDE MEASUREMENT

The extent to which cell lines differentiated from pre-adipocyte to mature adipocyte was determined by measuring Triglyceride accumulation. Oil Red O (Sigma-Aldrich) is a stain designed to stain lipids a bright red color. The following protocol was used to fix differentiated cell lines for Oil Red O staining: differentiated cells were washed twice with Phosphate-buffered saline (PBS) and fixed with 4% Paraformaldehyde (PFA) for one hour. Then PFA was removed and samples were washed once with PBS and once with H₂O. After that, cells were washed with 60% Isopropanol (in H₂O) and were allowed to sit for 5 minutes. Using freshly prepared 60% Oil Red Solution in H₂O,

which was filtered and sterilized using a 0.2µm syringe filter, cells were stained with solution and allowed to sit for 20 minutes. After staining is complete, cells were washed once with 60% Isopropanol and then again with H₂O twice. With the cells sitting in water, images were taken using a microscope.

The amount of triglyceride produced by each cell line was then quantified by washing cells three times with 60% Isopropanol (five minutes for each wash) and then extracting the oil red solution with 100% Isopropanol for five minutes. Using a 24-well plate, oil red was extracted using 50% of the well volume and 80% of the extraction volume (e.g. 200µL of extraction volume in 250µL of well volume). The absorbance was measured at 492 nm.

WESTERN BLOT ANALYSIS

Expression of proteins in each cell line was measured using the Western Blot technique (Bio Rad Technologies Protocol). The cells were washed with cold PBS and lysed using RIPA (Radio-immunoprecipitation assay) buffer containing 50mM Tris-HCl (pH 8.0), 150 mM NaCl, 1% Triton X-100, 0.5% sodium deoxycholate, 1mM sodium orthovanadate, 1mM NaF and a protease inhibitor cocktail. Cell suspensions were then placed in an Eppendorf tube and spun down in a centrifuge to separate proteins from other cell contents. The pellets at the bottom of the tubes were removed.

Protein samples were then subjected to a bicinchoninic acid (BCA) assay (Pierce Biotechnology Protocol) in order to determine the concentration of each sample. Equivalent concentrations of each protein sample were loaded onto and resolved on a

10% SDS-PAGE (Sodium Dodecyl Sulfate Polyacrylamide Gel Electrophoresis) gel, along with blue standard protein, a molecular weight marker.

After running the gel electrophoresis, transferring the separated proteins from the gel to Immobilon-PVDF membranes is achieved by assembling a transfer cassette and placing it into a transfer tank. The tank is filled with transfer buffer containing 25mM Tris, 190 mM glycine and 0.1% SDS (Thermo Scientific) and an electric current is applied (100v). The transfer is complete after approximately one hour.

PVDF membranes were washed with Phosphate-buffered Saline with Tween (PBST) once, blocked with 5% Bovine Serum Albumin (BSA) blocking buffer for one hour at room temperature and then incubated with primary antibodies overnight at 4 °C. The following day, membranes were washed with PBST three times and then incubated in horseradish peroxidase (HRP)-conjugated secondary antibodies for one hour at room temperature and washed with PBST three times. Membranes were developed by ECL kit (Millipore Corporation). Images of antibody incubation were analyzed using Bio Rad Imaging Lab software.

QUANTITATIVE POLYMERASE CHAIN REACTION (qPCR)

Quantitative Polymerase Chain Reactions, or qPCR, is a real-time reaction in which the target DNA is amplified using the enzyme reverse transcriptase. In order to determine if proteomic levels within cell lines, upon knockout of retromer's VPS35 subunit, were determined at a transcriptional level, a quantitative PCR analysis was performed.

Prior to performing qPCR on cell line samples, RNA must first be extracted and purified. The Qiagen Quick-Start Protocol kit was utilized in this process. Cells were harvested by adding approximately 350 μL of Buffer RLT (from kit) was directly to cell dishes. Samples were scraped off cell dishes and transferred into individual 1mL Eppendorf tubes to which 1 volume of 70% ethanol was added to the lysate. The lysate and ethanol were mixed by pipetting and were not centrifuged. Approximately 700 μL of sample, including any precipitate, was then transferred to an RNeasy Mini spin column placed in a 2mL collection tube (supplied by kit). The tubes were centrifuged for 15 seconds at 8000 rpm. Substances collected in the bottom 2mL collection tube were discarded.

700 μL of Buffer RW1 was added to RNeasy spin column and centrifuged for 15 seconds at 8,000 rpm. Flow-through was discarded. 500 μL of Buffer RPE was added to RNeasy spin column and centrifuged for 2 minutes at 8000 rpm. Flow-through was discarded. The RNeasy spin column was placed in a new 1.5mL collection tube (supplied). 30-50 μL of RNase-free water was added directly to the spin column membrane and centrifuged for 1 minute at 8,000 rpm to elute the RNA. The RNA concentration of each sample was determined using a Nano-drop machine (Thermo Fisher Scientific). The samples are now ready to undergo reverse transcription PCR to obtain its complementary DNA (cDNA).

Using Invitrogen's Retroscript kit (by Thermo Fischer Scientific), 2 μL of Random Decamers, 500 nanograms of RNA sample (calculated from concentrations obtained using Nano-drop machine) and enough RNase-free water to fill the sample tube

to 10 μ L were added to a new PCR tube. Each sample was placed in a PCR machine and was incubated for 8 minutes at 80°C.

After this reaction was completed, PCR tubes were removed and the following were added to each PCR sample tube: 2 μ L of RT buffer (from kit), 4 μ L of dNTP, 1 μ L RNase Inhibitor and 1 μ L of Reverse Transcriptase enzyme. The PCR tubes were incubated in the PCR machine for one hour at 92°C. The resulting cDNA can now be used for qPCR analysis.

Using a qPCR 96-well plate, the quantity of mRNA for the following proteins were analyzed: PPAR γ , AP2 α , Caveolin-1, GLUT4, VPS35, Actin and C/EBP β . According to the RNA primer library of Harvard University, it is unsure which RNA primer for C/EBP β will produce the desired results. Therefore, two different primers were used for experiments (will be referred to as C/EBP β #1 and C/EBP β #2). A master mix was prepared in which each well contained the following: 10 μ L of Syber detector (Bio Rad Technologies), 0.5 μ L of forward primer for DNA sequence of interest (Eurofin Genomics), 0.5 μ L of reverse primer for DNA sequence of interest (Eurofin Genomics) and 10 μ L of distilled H₂O. The master mix was mixed with 20 μ L of cDNA from each cell line. Each DNA sequence of interest was tested for three times so that the five cell lines being analyzed occupied 15 wells each for each forward/reverse primer used. Upon completion of qPCR analysis, results were measured against ribosomal protein 18S as a control.

Protein	Forward Primer (5' to 3')	Length/Tm (°F)	Reverse Primer	Length/Tm (°F)
PPAR γ	TCGCTGATGCACTGCCTATG	20/62.4	GAGAGGTCCACAGAGCTGATT	21/60.9
VPS35	GCTGTGAAGGTTTCAGTCATTCC	22/61.1	GTCAGGTAGACCTCCAAGTAGT	22/60.0
Actin	GGCTGTATCCCCTCCATCG	20/61.8	CCAGTTGGTAACAATGCCATGT	22/61.1
AP2 α	TTTTTCAGCTATGGACCGTCAC	22/60.6	GAAGTCGGCATTAGGGGTGTG	21/62.7
GLUT4	GTGACTGGAACACTGGTCCTA	21/60.8	CCAGCCACGTTGCATTGTAG	20/61.6
Caveolin-1	ATGTCTGGGGGCAAATACGTG	21/62.4	CGCGTCATACACTTGCTTCT	20/60.4
C/EBP β #1	AGTACAAGATGCGGCGCGA	22/62.4	CACCTTGTGCTGCGTCTCCA	20/63.0
C/EBP β #2	CAAGCTGAGCGACGAGTACAAG	19/61.5	AGCTGCTCCACCTTCTTCTGC	20/62.7

Table 1. Primers used for qPCR analysis

STATISTICAL ANALYSIS

Upon quantifying the results from the Oil-Red O, Western Blot and qPCR experiments, an ANOVA analysis of these results were performed and $p < 0.05$ was considered as statistically significant.

RESULTS

A total of nine experiments were completed in this study. The following results are a compilation of three experiments that were thought to be representative of this study.

SUCCESSFUL KNOCKDOWN OF VPS35 SUBUNIT

According to Western Blot and qPCR analyses, a successful knockdown of retromer's VPS35 subunit was achieved. This is demonstrated in Figure 7 below.

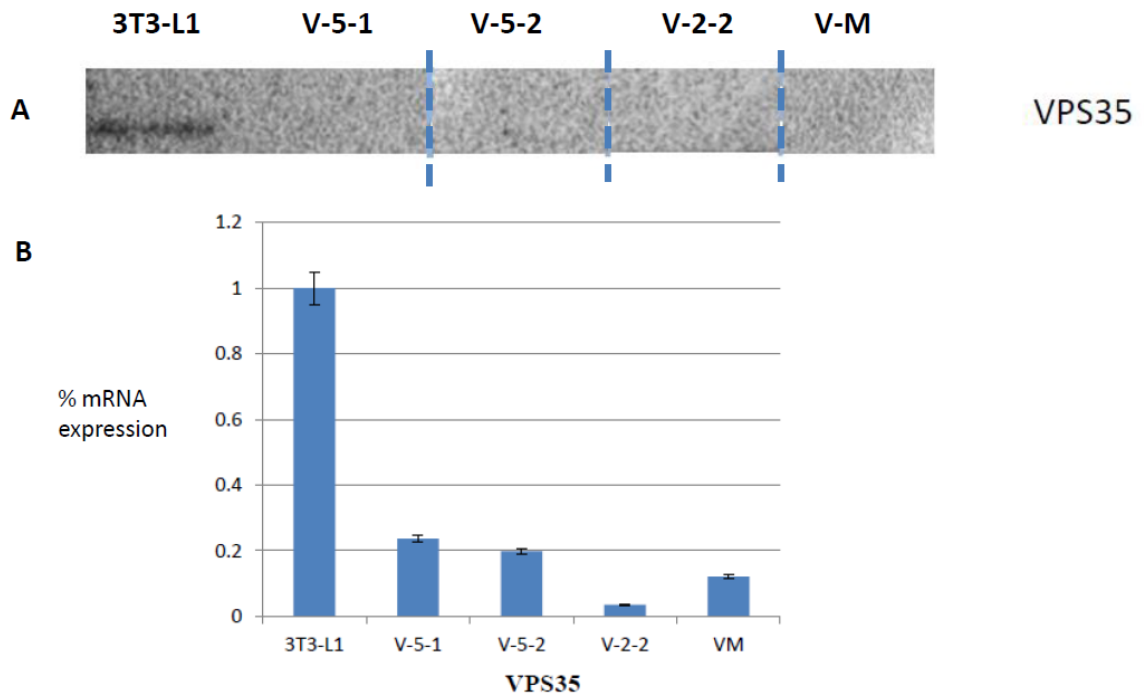


Figure 7. Successful knockdown of VPS35. A) Western Blot analysis. Note: Image has been rearranged as indicated by dashed lines. B) qPCR analysis. Relative to wild-type 3T3-L1 cell line, other cell lines have dramatically decreased mRNA expression of VPS35.

TRIGLYCERIDE ACCUMULATION

The extent to which VPS35 knockdown cell lines differentiated into mature adipocytes, compared to wild-type 3T3-L1 cells, was measured qualitatively using the Oil-Red O Stain (Sigma Aldrich). It was observed that compared to the wild-type 3T3-L1 cell line, the amount of triglycerides produced in each cell line from most to least is ranked in the following order: 3T3-L1, V-5-1, V-2-2, V-M and V-5-2. This is also demonstrated below in Figure 8.

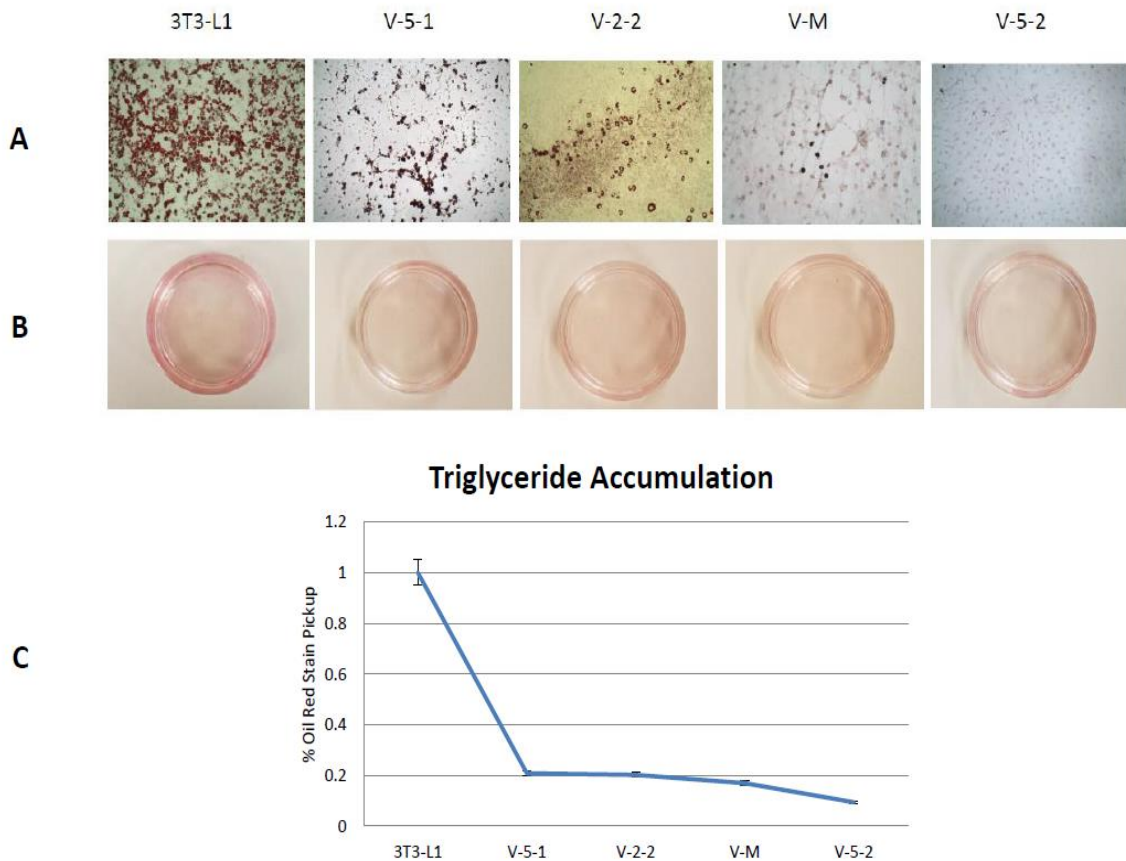


Figure 8. Level of Differentiation via Triglyceride Accumulation. A) Lipid droplets are stained in red. Microscopic images taken at 10x magnification B) Images of cell dishes taken at eye level C) Quantification of level of differentiation via Oil-Red O stain pickup. Error bars calculated using standard error.

Even though triglyceride accumulation is visible to the human eye with this staining, it is not possible to determine whether or not the knockout of retromer's VPS35 subunit is responsible for the increased triglyceride accumulation in V51 and V22 cell lines and decreased triglyceride accumulation in V52 and VM. The amount of triglyceride produced by each cell line was quantified (relative to wild-type 3T3-L1 adipocytes) and is shown above in Figure 8.

PROTEIN LEVELS OF VPS35 KNOCKDOWN CELL LINES

The effect of retromer on protein level expression was analyzed using Western Blots. Similar observations were made through Western Blot analysis as was made through Oil-Red O Staining. Antibodies were used to test for the presence of the pro-adipogenic markers PPAR γ , AP2 α , Caveolin-1, C/EBP β and GLUT4 in each cell line. Antibodies against β -Actin, a cytoskeletal protein, were used as a control to ensure that results were reflective of changes in adipocytes and not due to technical laboratory errors. The results are illustrated below.

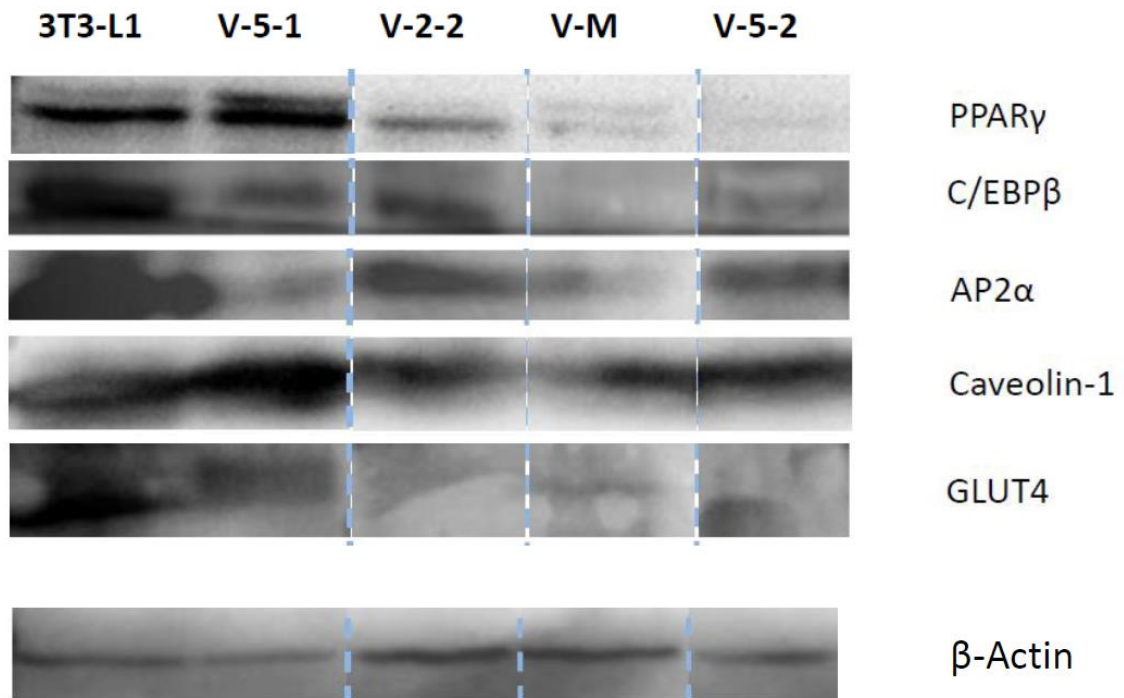


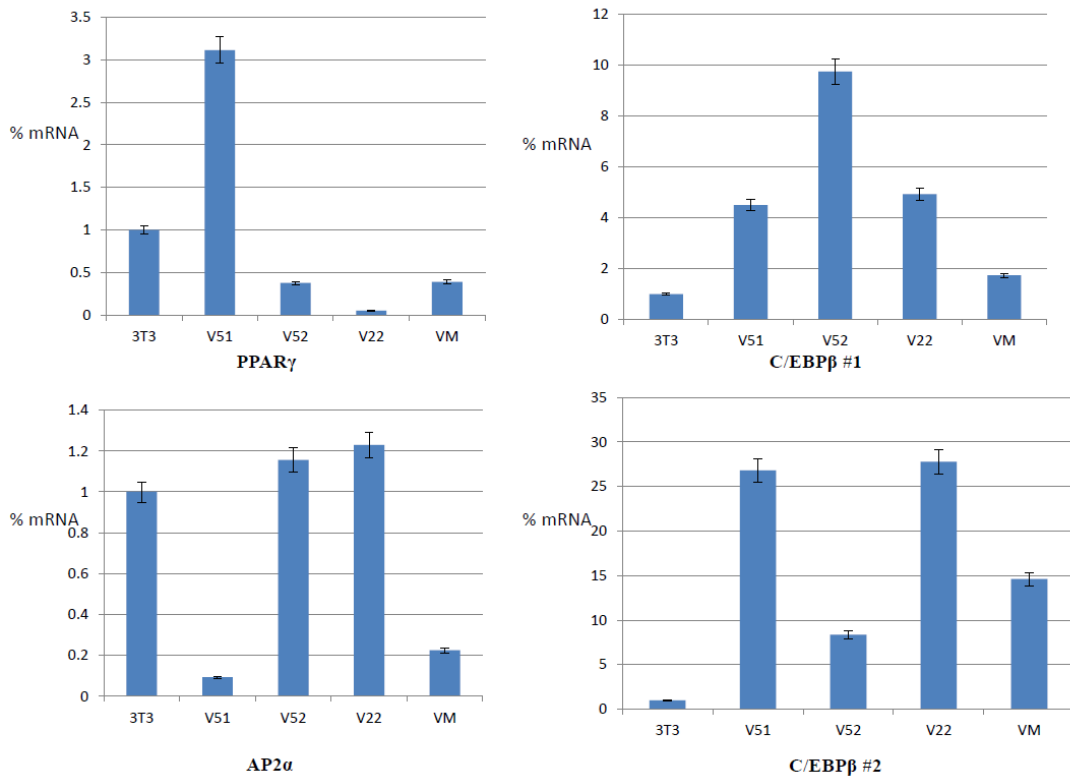
Figure 9. Protein Level Expression of Pro-adipogenic Markers in Differentiated Adipocytes. Western blot analyses are shown for two different sets of differentiated cells. Note: Images have been rearranged as demonstrated by the dashed lines.

Protein bands for Actin are relatively equal across all cell lines, indicating that there was little influence of technical laboratory error on results. Compared to wild-type 3T3-L1 cells, the amount of differentiation markers expressed, from highest to least, in cell lines is as follows: 3T3-L1, V-5-1, V-2-2, V-M and V-5-2. Interestingly, even though all knockdown cell lines differentiated worse than wild-type 3T3-L1 cells, the V-5-1 cell line expresses the most amount of protein for each marker, except for AP2 α . The V-2-2 cell line expresses the most AP2 α protein. In general, Oil-Red O staining and Western Blots have demonstrated that the higher the level of differentiation (according to number

of triglycerides produced), the higher the level of differentiation makers expressed, with the exception of levels of AP2 α expressed in V-2-2.

mRNA EXPRESSION OF VPS35 KNOCKDOWN CELL LINES

The effect of VPS35 knockdown on adipocytes was observed through qPCR analysis to determine if retromer acts at the transcriptional or translational level during the process of adipocyte differentiation. mRNA expression of pro-adipogenic markers were measured against ribosomal protein 18S as a control. The following graphs were obtained:



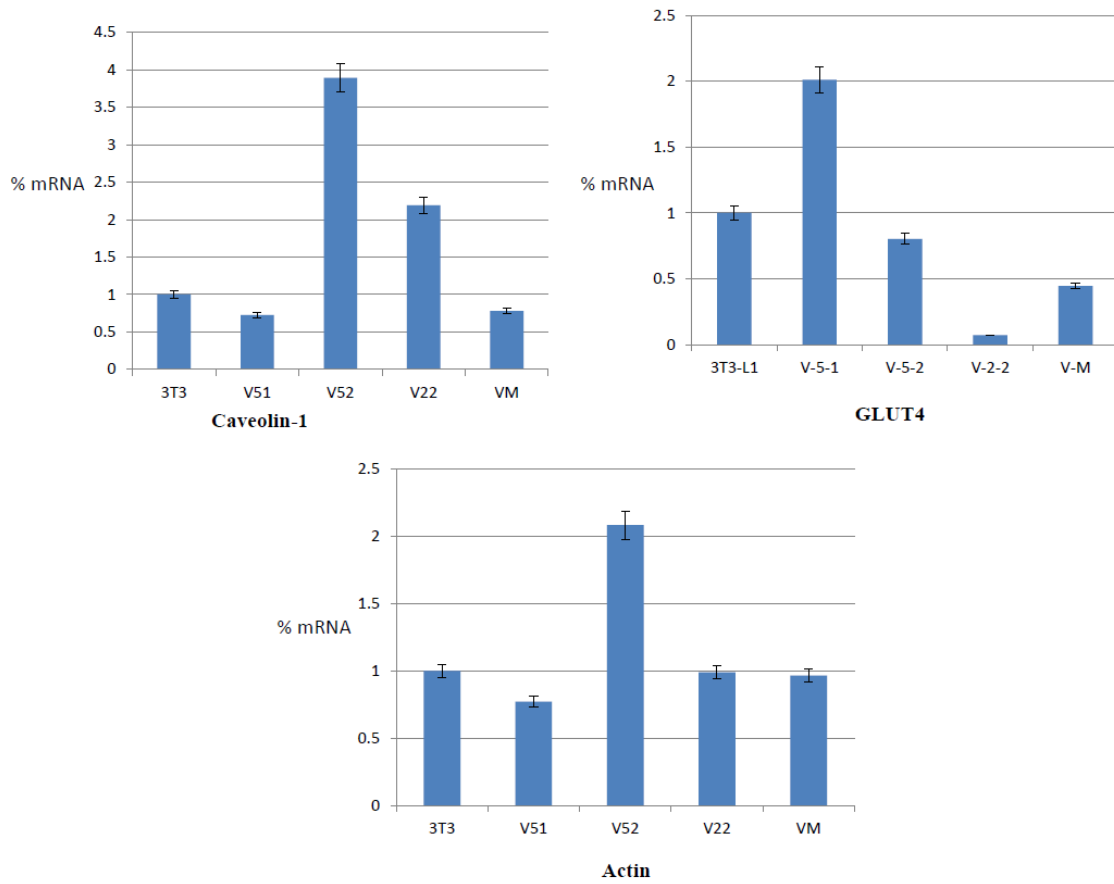
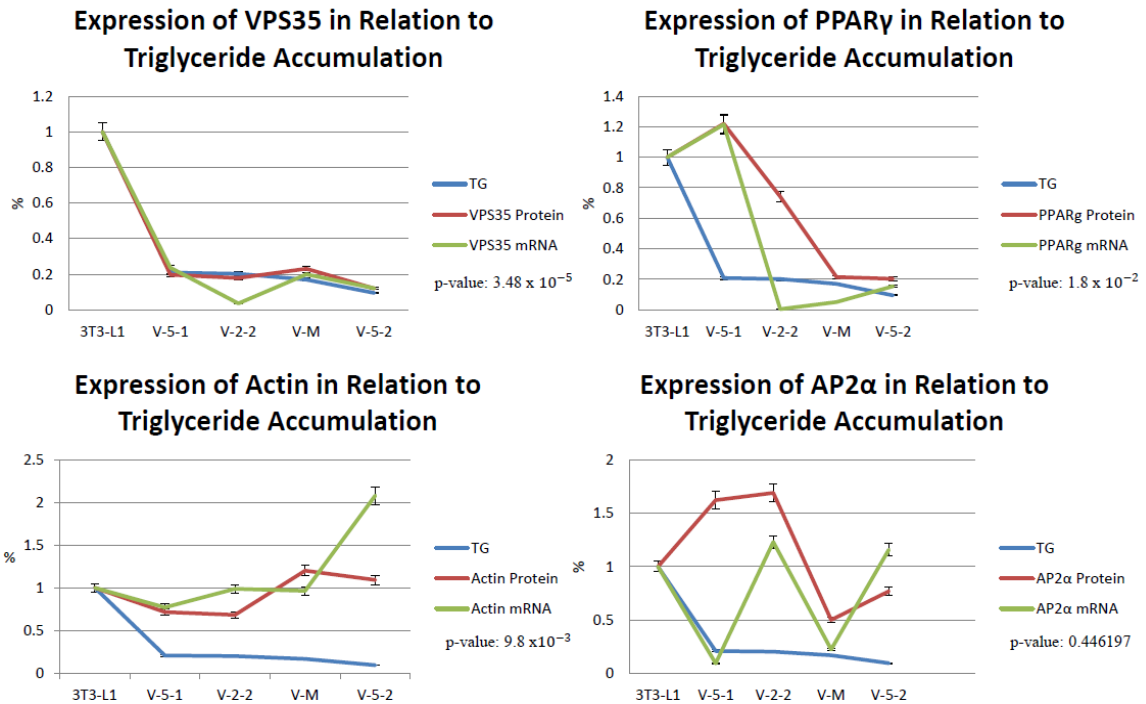


Figure 10. mRNA Expression of Pro-Adipogenic Markers in Differentiated Adipocytes. Error bars calculated using standard error.

As expected, the V-5-1 cell line displays the highest mRNA level for PPAR γ and GLUT4 and the V-2-2 cell line exhibits the highest mRNA level for AP2 α . However, there are discrepancies in data when considering Oil-Red O staining and Western Blots against qPCR data. Based on the above graphs, the V-5-2 cell line exhibits the highest mRNA level for Caveolin-1 and C/EBP β #1 even though this cell line has the lowest level of differentiation according to the Oil-Red O stains and Western Blot data. In addition, conflicting qPCR data was obtained for C/EBP β #1 and C/EBP β #2. The data for C/EBP β #2 is closer to the expected when considering Oil-Red O staining and Western Blot data.

DISCUSSION

According to the obtained results, it is clear that retromer plays a role in the differentiation of adipocytes at both the transcriptional and translational level. However, it is difficult to clearly define the exact role of retromer in the process of adipogenesis. All experimental data was compiled together in an effort to establish whether any relationship exists between retromer knockdown and the expression of pro-adipogenic markers and how this correlates with level of differentiation (Figure 11 below). Although the results of the Oil-Red O staining and the Western Blots agree with each other, the results of the qPCR data are where discrepancies arise (discussed below).



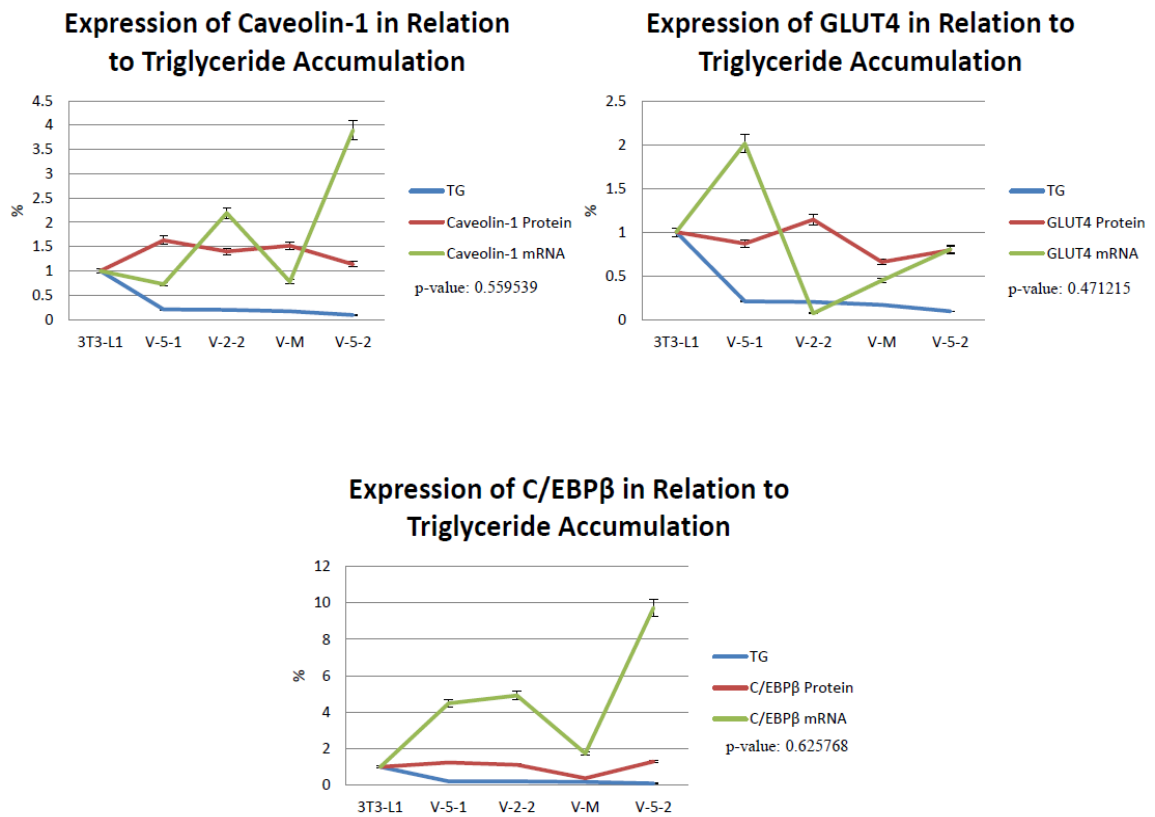


Figure 11. Comparison of Pro-Adipogenic Marker Expression in Relation to Triglyceride Accumulation. Error bars included and p-values indicated (versus control).

LEVEL OF DIFFERENTIATION CORRELATES WITH LEVEL OF TRIGLYCERIDE ACCUMULATION

Based on the results of the Oil-Red O experiment, it can be concluded that compared to the wild-type 3T3-L1 cell line, level of differentiation from best to worst is as follows: 3T3-L1, V-5-1, V-2-2, V-M and V-5-2. The order of differentiation from best to worst was further validated by measuring proteomic levels of differentiation markers

using Western Blot analyses. Due to the fact that Oil-Red O staining results and Western Blot results were consistent with each other, with the exception of differentiation marker AP2 α being most expressed in the V-2-2 cell line, it can be concluded that level of differentiation is positively correlated with triglyceride accumulation. Furthermore, quantification of Oil-Red O experiments were statistically significant ($p < 0.05$), further validating that level of differentiation positively correlates with triglyceride accumulation.

LEVEL OF DIFFERENTIATED IS CORRELATED WITH LEVEL OF DIFFERENTIATION MARKERS EXPRESSED

The Western Blot analyses show that the more differentiated the cell line is, as established by the amount of triglycerides produced, the more differentiation makers are expressed. V-5-2 is the worst differentiated cell line and expresses the least differentiation markers. V-5-1 is the most differentiated cell line and exhibits the most differentiation makers, except for AP2 α which is most expressed in V-2-2-, the second most differentiated cell line. The reason for this is uncertain. According to extraneous studies, exposure of pre-adipocytes to differentiating agents leads to the repression of AP2 α which is necessary for PPAR γ and C/EBP α gene expression (Farmer et al., 2006; Morrison & Farmer et al., 2000). However, as observed in the Western Blot analyses of this study, V-2-2 expresses high levels of both PPAR γ and AP2 α (relative to wild-type 3T3-L1 cells), which is contradictory and might suggest that VPS35 knockdown may act at the transcriptional level of AP2 α .

Furthermore, according to Figure 11, significant $p < 0.05$ were obtained for VPS35, PPAR γ and Actin but $p > 0.05$ were obtained for AP2 α , Caveolin-1, GLUT4 and C/EBP β . This could be due to experimental error or it could be that VPS35 knockdown does not have an effect on the expression of these pro-adipogenic markers. Percentage of protein levels expressed, in comparison to wild-type 3T3-L1 cells, are calculated below in Table 2.

Cell Line	PPAR γ	C/EBP β	AP2 α	GLUT4	Caveolin-1	β -Actin
V-5-1	1 + .22	1 + .24	1 + .62	1 - .13	1 + .63	1 - .28
V-2-2	1 - .26	1 + .12	1 + .69	1 + .14	1 + .41	1 - .32
V-M	1 - .79	1 - .62	1 - .49	1 - .34	1 + .52	1 + .20
V-5-2	1 - .79	1 + .30	1 - .23	1 - .21	1 + .14	1 + .09

Table 2. Percentage of Protein Levels Expressed. Percentages were calculated in comparison to wild-type 3T3-L1 cells (assuming 3T3-L1 expresses protein at 100%).

DOES EXPRESSION OF DIFFERENTIATION MAKERS CORRELATE WITH LEVELS OF COGNATE mRNA?

Although proteomic levels of differentiation markers positively correlates with triglyceride accumulation, the precise role of VPS35 knockdown is not as clear when examining the mRNA expression of key differentiation markers. As expected, mRNA expression of VPS35 is the highest in the wild-type 3T3-L1 cell line and much lower in

the VPS35 knockdown cell lines. Therefore, the V-5-1, V-5-2, V-2-2 and V-M are truly VPS35 knockdown cell lines. In addition, mRNA expression of differentiation markers PPAR γ and GLUT4 are the highest in the V-5-1 cell line and mRNA expression of AP2 α is the highest in the V-2-2 cell line, agreeing with the Western Blot analyses.

Interestingly, level of mRNA expression of PPAR γ and AP2 α were the opposite of each other in each cell line, which is consistent with the observation that repression of AP2 α levels allows for the gene expression of PPAR γ (Farmer et al., 2006; Morrison & Farmer et al., 2000). However, it is uncertain why this transcriptional event does not also present itself at the translational level. The mRNA expression of AP2 α in relation to triglyceride accumulation was also statistically insignificant ($p > 0.05$), indicating experimental error or there is no correlation with VPS35 knockdown.

Furthermore, it has been previously established in extraneous studies that as cells undergo morphological changes, the level of actin expressed decreases to allow for the proper formation of mature adipocytes. According to the results of this particular study, mRNA expression of actin is the highest in V-5-2, supporting the observation that this cell line differentiates the worst, and the lowest in V-5-1, supporting the observation that this cell line differentiates the best. Thus far, there is a correlation of retromer knockdown and active mRNA level of differentiation markers, ultimately altering the process of differentiation for these cells.

However, mRNA expression of Caveolin-1 is not most expressed in V-5-1 as expected, but instead is most expressed in V-5-2. In addition, the results of the mRNA expression of C/EBP β #1 and C/EBP β #2 differ significantly. Although two different

primers were used to test for this differentiation marker, the results should be more similar than different. In this study, C/EBP β #1 mRNA expression is highest for V-5-2 and the lowest for 3T3-L1, suggesting that the wild-type cells differentiated the worst and is not supported by any other data collected in this study. mRNA expression for C/EBP β #2 is highest in V-2-2 and second highest in V-5-1. The results for C/EBP β #2 are closer to expected. The differing results between both C/EBP β primers are most likely due to technical error and warrant a repeated qPCR analysis. In addition, $p > 0.05$ were obtained for mRNA expression of Caveolin-1 and C/EBP β which may suggest there is no correlation with VPS35 knockdown.

KNOCKDOWN OF VPS35 AFFECTS THE ADIPOGENESIS PROCESS

An average of all Western Blot experiments and qPCR experiments were compiled and normalized against the wild-type 3T3-L1 cell line. According to Figure 11, it is clear that there is a correlation between the knockdown of VPS35 and the amount of triglycerides produced by adipocytes ($p < 0.05$). Therefore, it can be safely concluded that a fully functional VPS35 subunit is necessary for retromer to facilitate the adipogenesis process.

MECHANISM OF ACTION FOR RETROMER IN ADIPOGENESIS REMAINS ELUSIVE

Based on the results of this study, level of differentiation appears to be correlated with VPS35 knockdown, however it is interesting to note that the knockdown of retromer's VPS35 subunit has different effects in each cell line. VPS35 knockdown is positively correlated in the V-5-2- and V-M cell lines, or knockdown downregulates adipocyte differentiation, whereas VPS35 knockdown is negatively correlated in the V-5-1 and V-2-2 cell lines, or knockdown upregulated adipocyte differentiation.

These differing effects of retromer knockdown could be due to the different gRNAs used when creating these VPS35 knockdown cell lines. V-2-2 and V-M cell lines contain different gRNAs and different effects on adipocyte differentiation were observed. However, the same gRNA was used to create the V-5-1 and V-5-2 cell lines, but V-5-1- differentiated the best and V-5-2- differentiated the worst (compared to wild-type 3T3-L1).

A potential reason for the differing results between the V-5-1 and V-5-2 cell line, despite these two cell lines containing the same gRNA, could be the time necessary for full differentiation of adipocytes to occur. Not much activity was observed at the translational level; however, qPCR analyses reveal that mRNA expression of C/EBP β and GLUT4 are higher in the V-5-2 cell line than in the V-2-2 cell line. V-5-2 and V-2-2 also express similar mRNA levels of AP2 α and yet, V-2-2 differentiates much better than V-5-2. It is reasonable to believe that V-5-2 has the potential to differentiate into

functionally mature adipocytes if given more than the eight to ten days that was given to all cell lines in this study. This phenomenon requires further analysis.

FUTURE IMPLICATIONS

It is clear retromer plays a role in adipogenesis, however retromer's mechanism of action remains unclear. Based on the results of this study, both cases of upregulation and downregulation of adipocyte differentiation were observed. Therefore, it cannot be concluded whether there is a positive correlation between retromer and adipocyte differentiation (retromer knockout results in impaired differentiation) or if there is a negative correlation (retromer knockout upregulates differentiation at a level higher than normal). Due to the fact that knockdown of retromer did result in impaired adipocyte differentiation in some cases, resulting in lower levels of essential proteins expressed, such as GLUT4, it is possible that retromer does not play a direct role in the onset of Diabetes Mellitus. Instead, there could be an indirect role that retromer plays in adipogenesis that was not analyzed in this study. This could be a potential avenue of research for metabolic diseases such as Type II Diabetes.

REFERENCES

- Bean, B. D. M., Davey, M., & Conibear, E. (2017). Cargo selectivity of yeast sorting nexins. *Traffic*, *18*(2), 110–122. <https://doi.org/10.1111/tra.12459>
- Bogan, J. S., & Kandror, K. V. (2010). Biogenesis and regulation of insulin-responsive vesicles containing GLUT4. *Current Opinion in Cell Biology*, *22*(4), 506–512. <https://doi.org/10.1016/j.ceb.2010.03.012>
- Collins, B. M. (2008). The Structure and Function of the Retromer Protein Complex. *Traffic*, *9*(11), 1811–1822. <https://doi.org/10.1111/j.1600-0854.2008.00777.x>
- Collins, B. M., Norwood, S. J., Kerr, M. C., Mahony, D., Seaman, M. N. J., Teasdale, R. D., & Owen, D. J. (2008). Structure of Vps26B and Mapping of its Interaction with the Retromer Protein Complex. *Traffic*, *9*(3), 366–379. <https://doi.org/10.1111/j.1600-0854.2007.00688.x>
- Cullen, P. J., & Korswagen, H. C. (2012). Sorting nexins provide diversity for retromer-dependent trafficking events. *Nature Cell Biology*, *14*(1), 29–37. <https://doi.org/10.1038/ncb2374>
- Ding, Y., Li, H., Chen, L.-L., & Xie, K. (2016). Recent Advances in Genome Editing Using CRISPR/Cas9. *Frontiers in Plant Science*, *7*. <https://doi.org/10.3389/fpls.2016.00703>
- Farmer, S. R. (2006). Transcriptional control of adipocyte formation. *Cell Metabolism*, *4*(4), 263–273. <https://doi.org/10.1016/j.cmet.2006.07.001>

- Gallon, M., & Cullen, P. J. (2015). Retromer and sorting nexins in endosomal sorting. *Biochemical Society Transactions*, 43(1), 33–47.
<https://doi.org/10.1042/BST20140290>
- Guo, L., Li, X., & Tang, Q.-Q. (2015). Transcriptional Regulation of Adipocyte Differentiation: A Central Role for CCAAT/Enhancer-binding Protein (C/EBP) β . *Journal of Biological Chemistry*, 290(2), 755–761.
<https://doi.org/10.1074/jbc.R114.619957>
- Hammarstedt, A., Andersson, C. X., Sopasakis, V. R., & Smith, U. (2005). The effect of PPAR γ ligands on the adipose tissue in insulin resistance. *Prostaglandins, Leukotrienes and Essential Fatty Acids*, 73(1), 65–75.
<https://doi.org/10.1016/j.plefa.2005.04.008>
- Kimura, N., Samura, E., Suzuki, K., Okabayashi, S., Shimosawa, N., & Yasutomi, Y. (2016). Dynein Dysfunction Reproduces Age-Dependent Retromer Deficiency. *The American Journal of Pathology*, 186(7), 1952–1966.
<https://doi.org/10.1016/j.ajpath.2016.03.006>
- Lucas, M., Gershlick, D. C., Vidaurrazaga, A., Rojas, A. L., Bonifacino, J. S., & Hierro, A. (2016). Structural Mechanism for Cargo Recognition by the Retromer Complex. *Cell*, 167(6), 1623–1635.e14. <https://doi.org/10.1016/j.cell.2016.10.056>
- Ma, J., Nakagawa, Y., Kojima, I., & Shibata, H. (2014). Prolonged Insulin Stimulation Down-regulates GLUT4 through Oxidative Stress-mediated Retromer Inhibition by a Protein Kinase CK2-dependent Mechanism in 3T3-L1 Adipocytes. *Journal*

of Biological Chemistry, 289(1), 133–142.

<https://doi.org/10.1074/jbc.M113.533240>

Ma, X., Lee, P., Chisholm, D. J., & James, D. E. (2015). Control of Adipocyte Differentiation in Different Fat Depots; Implications for Pathophysiology or Therapy. *Frontiers in Endocrinology*, 6.

<https://doi.org/10.3389/fendo.2015.00001>

Maier, V. H., & Gould, G. W. (2000). Long-term insulin treatment of 3T3-L1 adipocytes results in mis-targeting of GLUT4: implications for insulin-stimulated glucose transport. *Diabetologia*, 43(10), 1273–1281.

<https://doi.org/10.1007/s001250051523>

Morrison, R. F., & Farmer, S. R. (2000). Hormonal Signaling and Transcriptional Control of Adipocyte Differentiation. *The Journal of Nutrition*, 130(12), 3116S–3121S.

Rosen, E. D., Sarraf, P., Troy, A. E., Bradwin, G., Moore, K., Milstone, D. S., ...

Mortensen, R. M. (1999). PPAR γ Is Required for the Differentiation of Adipose Tissue In Vivo and In Vitro. *Molecular Cell*, 4(4), 611–617.

[https://doi.org/10.1016/S1097-2765\(00\)80211-7](https://doi.org/10.1016/S1097-2765(00)80211-7)

Sadigh-Eteghad, S., Askari-Nejad, M. S., Mahmoudi, J., & Majdi, A. (2016). Cargo trafficking in Alzheimer's disease: the possible role of retromer. *Neurological Sciences*, 37(1), 17–22. <https://doi.org/10.1007/s10072-015-2399-3>

Sander, J. D., & Joung, J. K. (2014). CRISPR-Cas systems for genome editing, regulation and targeting. *Nature Biotechnology*, 32(4), 347–355.

<https://doi.org/10.1038/nbt.2842>

- Seaman, M. N. J. (2012). The retromer complex – endosomal protein recycling and beyond. *J Cell Sci*, *125*(20), 4693–4702. <https://doi.org/10.1242/jcs.103440>
- Shi, J., & Kandror, K. V. (2005). Sortilin Is Essential and Sufficient for the Formation of Glut4 Storage Vesicles in 3T3-L1 Adipocytes. *Developmental Cell*, *9*(1), 99–108. <https://doi.org/10.1016/j.devcel.2005.04.004>
- Siersbæk, R., Nielsen, R., & Mandrup, S. (2010). PPAR γ in adipocyte differentiation and metabolism – Novel insights from genome-wide studies. *FEBS Letters*, *584*(15), 3242–3249. <https://doi.org/10.1016/j.febslet.2010.06.010>
- Steinberg, F., Gallon, M., Winfield, M., Thomas, E., Bell, A. J., Heesom, K. J., ... Cullen, P. J. (2013). A global analysis of SNX27-retromer assembly and cargo specificity reveals a function in glucose and metal ion transport. *Nature Cell Biology*, *15*(5), 461–471. <https://doi.org/10.1038/ncb2721>
- Trousdale, C., & Kim, K. (2015). Retromer: Structure, function, and roles in mammalian disease. *European Journal of Cell Biology*, *94*(11), 513–521. <https://doi.org/10.1016/j.ejcb.2015.07.002>
- Ullah, I., Subbarao, R. B., & Rho, G. J. (2015). Human mesenchymal stem cells - current trends and future prospective. *Bioscience Reports*, *35*(2). <https://doi.org/10.1042/BSR20150025>
- Insulin Signaling Transduction Pathway. (n.d.). Retrieved from <http://www.gbpuat-cbsh.ac.in/departments/bi/database/phytodiabcare/4%20headings%20of%20insulin/Insulin%20pathway.html>

- Wang, X., Huang, X., Fang, X., Zhang, Y., & Wang, W. (2016). CRISPR-Cas9 System as a Versatile Tool for Genome Engineering in Human Cells. *Molecular Therapy - Nucleic Acids*, 5, Article e388. <https://doi.org/10.1038/mtna.2016.95>
- Wu, L.-G., Hamid, E., Shin, W., & Chiang, H.-C. (2014). Exocytosis and Endocytosis: Modes, Functions, and Coupling Mechanisms. *Annual Review of Physiology*, 76, 301–331. <https://doi.org/10.1146/annurev-physiol-021113-170305>
- Yamanaka, S. (2008). Induction of pluripotent stem cells from mouse fibroblasts by four transcription factors. *Cell Proliferation*, 41, 51–56. <https://doi.org/10.1111/j.1365-2184.2008.00493.x>
- Yang, Z., Hong, L. K., Follett, J., Wabitsch, M., Hamilton, N. A., Collins, B. M., ... Teasdale, R. D. (2016). Functional characterization of retromer in GLUT4 storage vesicle formation and adipocyte differentiation. *The FASEB Journal*, 30(3), 1037–1050. <https://doi.org/10.1096/fj.15-274704>
- Zhang, Q.-Y., Tan, M.-S., Yu, J.-T., & Tan, L. (2016). The Role of Retromer in Alzheimer's Disease. *Molecular Neurobiology*, 53(6), 4201–4209. <https://doi.org/10.1007/s12035-015-9366-0>
- Zhao, X., Nothwehr, S., Lara-Lemus, R., Zhang, B., Peter, H., & Arvan, P. (2007). Dominant-Negative Behavior of Mammalian Vps35 in Yeast Requires a Conserved PRLYL Motif Involved in Retromer Assembly. *Traffic (Copenhagen, Denmark)*, 8(12), 1829–1840. <https://doi.org/10.1111/j.1600-0854.2007.00658.x>

CURRICULUM VITAE

